American Journal of Earth and Environmental Sciences
2018; 1(2): 71-81
http://www.aascit.org/journal/eas

American Association for Science and Technology

Evaluation of Atmospheric Stability Categories from Gradient Richardson Number in Jos, North Central Nigeria

David Onojiede Edokpa[1], Precious Nwobidi Ede[2]

[1]Department of Geography and Environmental Management, University of Port Harcourt, Port Harcourt, Nigeria
[2]Institute of Geosciences and Space Technology, Rivers State University of Science and Technology, Port Harcourt, Nigeria

Email address

onojiede@gmail.com (D. O. Edokpa), onodavee@yahoo.com (D. O. Edokpa), preciousede@ust.ng (P. N. Ede)

Citation

David Onojiede Edokpa, Precious Nwobidi Ede. Evaluation of Atmospheric Stability Categories from Gradient Richardson Number in Jos, North Central Nigeria. *American Journal of Earth and Environmental Sciences.* Vol. 1, No. 2, 2018, pp. 71-81.

Received: February 5, 2018; **Accepted**: March 1, 2018; **Published**: April 27, 2018

Abstract: This study surveyed the levels of atmospheric stability across the atmospheric boundary layer in Jos, north-central Nigeria. Five years (2011-2015) meteorological data for temperature and wind speed at 1000mbar pressure level was retrieved and processed from ECMWF Era-Interim Re-analysis platform. The data were for 6-hourly synoptic hours: 0000H, 0600H, 1200H and 1800H at 0.125° grid resolution. The gradient Richardson (R_{ig}) number technique was used to assess stability conditions across distinct layers: 10-50m (surface layer); 50-100m (mid layer) and 100-1300m (upper layer). Results indicated that the surface layer is always in unstable state as over 90% and 100% of R_{ig} values were below Richardson Critical (R_{ic}) value of 0.25 and Richardson Termination level (R_T) of 1, respectively. Stable conditions exist at the mid layer across the hours and all R_{ig} values were greater than R_T level of 1. R_{ig} values for the upper layer were largely negative and ranged between -52 to -360. This indicates very strong unstable conditions. Atmospheric stability generated through mixed convection prevailed at the surface layer and upper layer but with more of forced and free convection. This shows that mechanical turbulence is dominant at the surface while thermal buoyancy prevails at the upper level. Linking results to emission dispersion proposes that air pollutants will be dispersed across far and near expanses at the upper layer and surface layers. This is due to the laminar pattern of the mid layer that will restrict altitudinal and horizontal emission dispersion. Authorities should certify that prospective emission sources are above 50m to safeguard the health of sensitive receptors as regards emissions concentrations. Also, wind energy could be utilised as surface R_{ig} values concur with obtainable wind shear values.

Keywords: Atmospheric Stability, Gradient Richardson Number, Boundary Layer, Jos, Emissions

1. Introduction

Atmospheric stability entails the vertical alteration of air masses which strongly depend on the altitudinal changes of air temperature – a phenomenon so vital for the survival of boundary layer dwellers when related to pollutants dispersion within the planetary layer. Atmospheric stability specifies the deviation of diverse atmospheric variables at various altitudinal heights and consequently the presence of diverse horizontal layers and the degree of mixing exhibited by these layers [1]. Several researches have revealed the pattern and degree of atmospheric stability situations across spatial locations [2-5]. Stability categories exist in three major forms, namely: unstable, neutral and stable conditions. The prevalence of these conditions is based on the alteration of temperature with height termed, 'lapse rate'. The Pasquill-Gifford (P-G) stability scheme designed in 1961 classified these major stability categories into six different classes (A-F) with 'A-C' and 'D-F' emphasizing the unstable and neutral-stable conditions, respectively. In relation to evaluating stability pattern across layers in the atmospheric boundary layer (ABL), two universally accepted stability parameters are recommended [6] i.e. the Obukhov Length and the Richardson number. The Obukhov Length involves the determination of surface heat fluxes to assess the degree of stability conditions, while the Richardson number demands the evaluation of meteorological variables such as wind velocity and air temperature at two vertical levels in order to determine altitudinal stability variations. What makes Richardson number more suitable than Monin-

Obukhov length (L), is that 'L' is more effective to the surface boundary layer (i.e. 0-50m) due to the strong effect of surface heat fluxes. These heat fluxes dissipate as one move away from the surface. The main advantage of the Richardson number is that, either the mechanical or thermal aspect of the dimensionless scheme within or above the surface layer could influence stability pattern across sub-layers. The core difference between the P-G stability scheme and the Richardson number method is that the former evaluates the stability of the atmospheric boundary layer as one column under a unified total cloud cover while the latter examines the existence of stability variation within sub-layers in the atmospheric boundary layer. It is known [7] that the atmospheric boundary layer exists in two states: laminar and turbulent boundary layers. The laminar pattern is associated with the stable-neutral stability phase which inhibits emission dispersion; while the turbulent pattern is associated with the unstable stability phase which enhances emission dispersion. It has been specified by [8] and [9] that the turbulent state of the ABL determines the degree of mixing that either increases or reduces the ABL height. The laminar state of the atmosphere restricts mixing and creates levels of stable conditions. The ABL could stretch beyond 1km during the day and shrinks to below 100m at night [10].

This paper provides the atmospheric stability regime of Jos metropolis from Gradient Richardson number estimations across sub-layers within the atmospheric boundary layer i.e. 0-50m; 50-100m and 100-1300m for the surface, mid and upper layers concurrently.

2. The Study Area

Jos is a city situated in north-central Nigeria, the capital of Plateau State. It is located at an elevation of 1285m above sea level [11] and lies between Latitude 9° 33′ N to 9° 55′ N and Longitude 8° 44′ E to 9° 10′ E of the equator. The area is sited in the Montane vegetation region of Nigeria influenced by a relatively high altitude climate. Jos has the tropical continental climate classified as Koppen's *Aw* and lies on the divide of the bimodal rainfall regime which peaks in July and September. Average annual rainfall for the area ranges between 1200-1500mm with wet and dry spells covering May to October and November to April, respectively [12]. The period of dry spell is ravaged by dust haze with deposits of aerosols flown from the Sahara desert. Average annual maximum and minimum temperatures ranges between 24-31°C and 12-18°C respectively with March/April being the warmest months and July/August being the coolest months. Relative humidity varies between 22-73% with lower and higher values recorded during the periods of dry and rainy seasons [13]. The mean wind speed range for the city according to [14] is about 5.2m/s. Wind speed is generally high during the day and low during night time. Also, higher wind speeds dominate slightly during the dry season than in the rainy period (Figures 2-5). Wind direction for the area is predominantly westerly in the rainy season and easterly in the dry season.

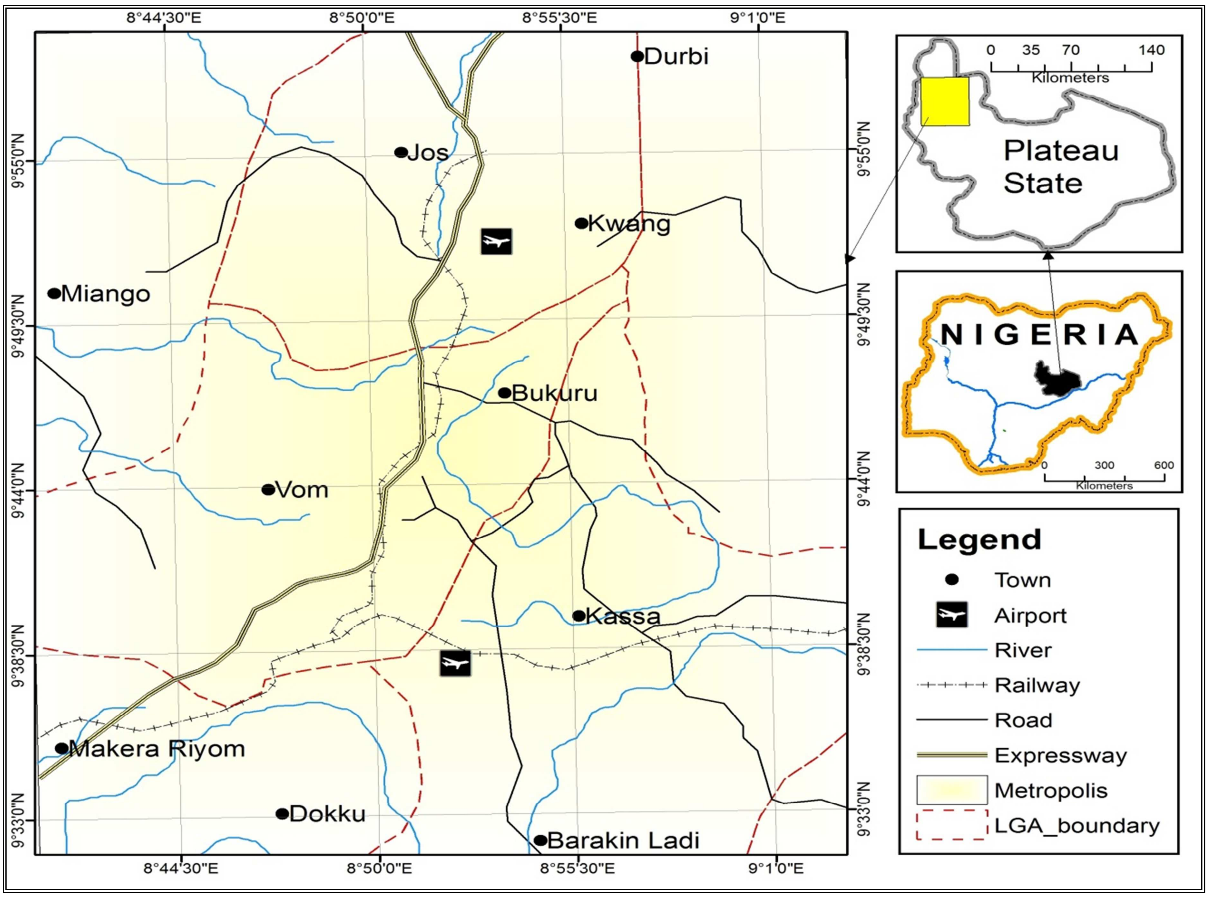

Figure 1. *Map Showing Study Area.*

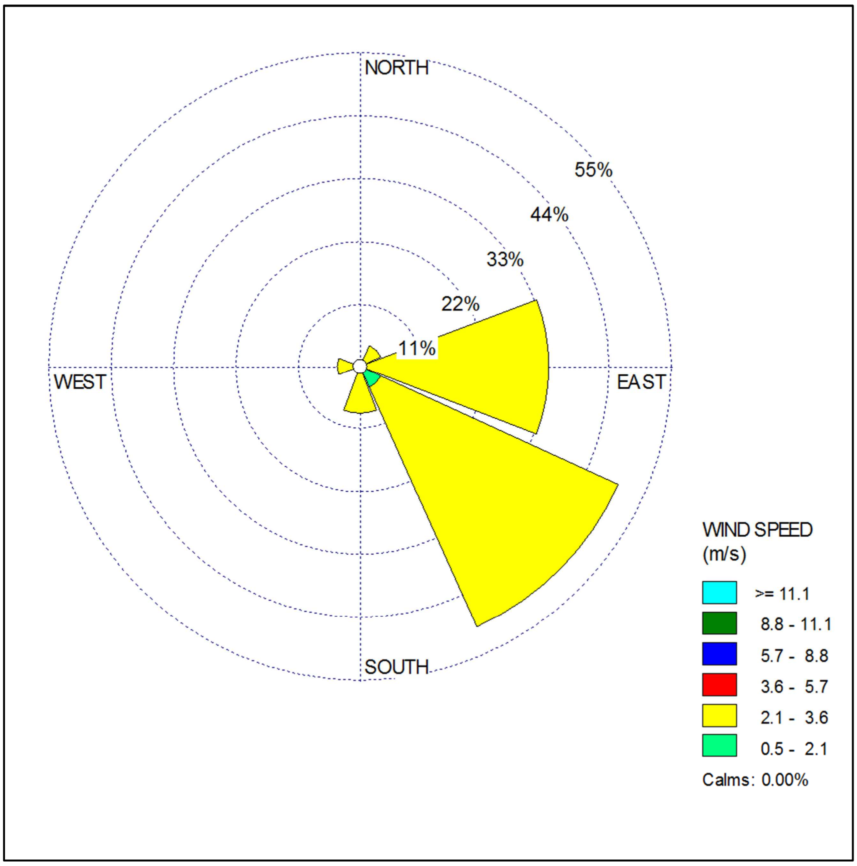

Figures 2. *Wind velocity/direction Pattern at 0000Hr in Jos from December-February.*

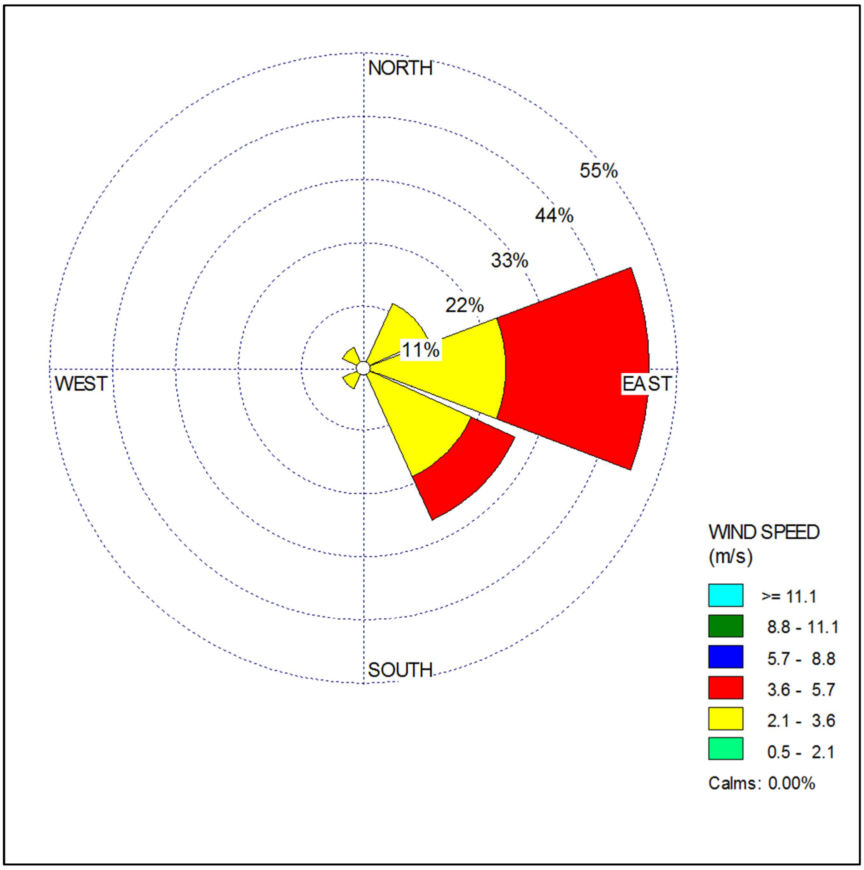

Figures 3. *Wind velocity/direction Pattern at 1200Hr in Jos from December-February.*

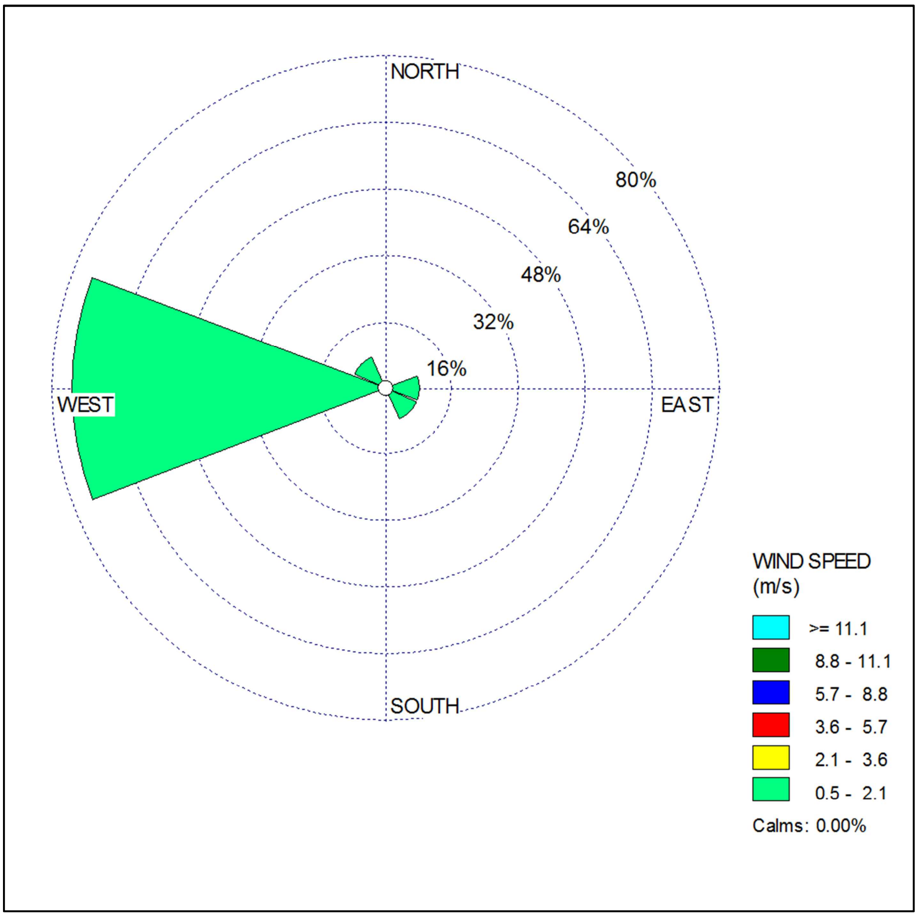

Figures 4. *Wind velocity/direction Pattern at 0000Hr in Jos from June-August.*

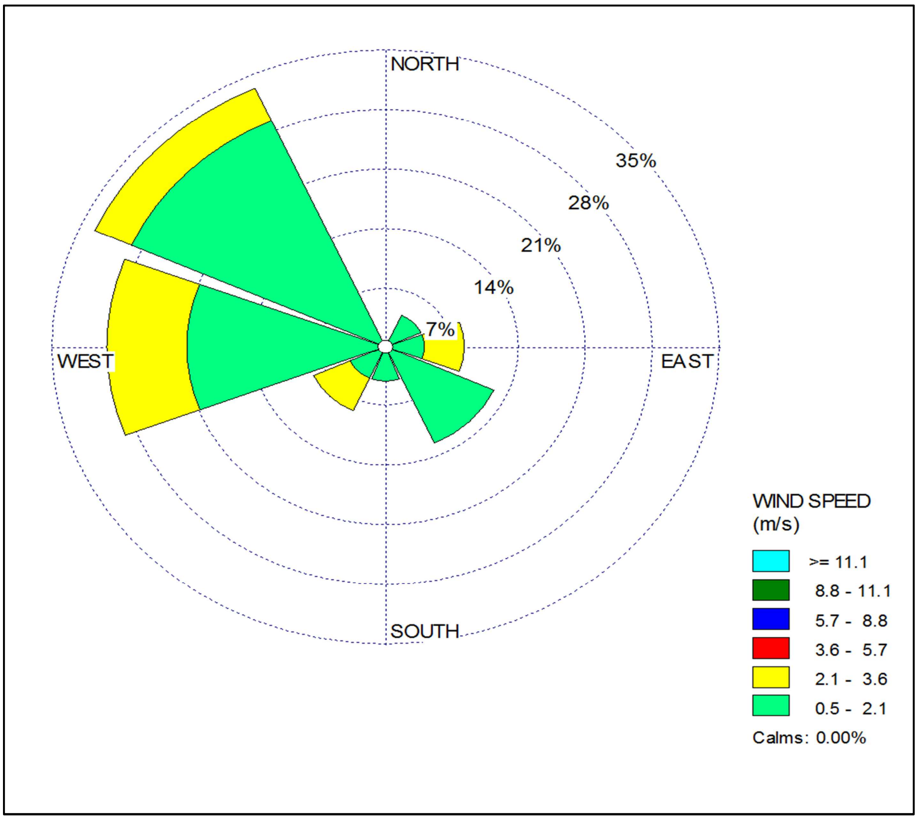

Figures 5. *Wind velocity/direction Pattern at 1200Hr in Jos from June-August.*

3. Data and Methodology

3.1. Data

The data utilised for this research were retrieved from the European Centre for Medium Ranged Weather Forecast (ECMWF) Era-Interim Re-analysis data for the period 2011 to 2015. The ECMWF's database is the modernised and most prevalent atmospheric reanalysis data that has proven to be useful in the investigation of the West African climatic system. The utilisation of the upgraded reanalysis data has surpassed predictions and articulates progressive assessments about the accomplishments in the examination of weather data comprehended within the last decade. The data were obtained at 0.125 latitudinal and longitudinal degree resolution at 6-hourly synoptic interval, i.e., 0000, 0600, 1200 and 1800. Meteorological variables such as wind speed, air temperature and relative humidity were acquired at pressure level of 1000mbar.

3.2. Methodology

There are various techniques of assessing stability conditions: these include the Richardson number (R_i), Monin-Obukhov Length (L), temperature gradient, wind speed gradient, lapse rate method, etc., however, the Richardson number and P-G technique are widely used and are acceptable due to their simplicity and applicability [15]. According to [16], when meteorologist use the conversional term of Richardson number (R_i); what is being referred to, is the Gradient Richardson number (R_{ig}). The difference between the bulk (R_{ib}) and gradient (R_{ig}) Richardson numbers is that the former uses one level surface temperature for analysis while the latter utilises gradient temperature at two levels for stability analysis [1]. The tendency for available meteorological data usage gives the P-G scheme as well as the Richardson number method an edge over other techniques of assessing atmospheric stability. This research uses the gradient Richardson number to evaluate the degree of stability conditions across three layers (10-50m, 50-100m and 100-1300m). The relationship between the Richardson number and the Monin-Obukhov length (L) was used to estimate the approximate altitudinal height where free convection displaces forced ascents of air mass. MATLAB software was utilised in analysing the mathematical equations.

3.2.1. Analysis of Gradient Richardson Number (R_{ig})

The gradient Richardson number (R_{ig}) relates the dimensionless ratio of the rate of work done by buoyancy forces divided by the mechanical production of turbulence. As analysed in [7], it is given by:

$$R_{ig} = \frac{\frac{g}{\theta}[\frac{\partial \theta}{\partial z}]}{[(\frac{\partial U}{\partial z})^2 + ((\frac{\partial v}{\partial z})^2]} \tag{1}$$

Where,

g is the gravitational acceleration (m/s^2)

θ is the potential temperature

u and v, is the east-west and north south components of the winds respectively (m/s^2).

z is the vertical height (m).

The u and v wind components is resolved into the mean wind speed $(d\hat{u}/dz)^2$ and given as

$$(d\hat{u}/dz)^2 = \frac{\Delta \hat{u}}{Z_m \ln(Z_2/Z_1)} \tag{2}$$

Where z_m is the mean vertical height considered. The relationship between Monin-Obukhov Length and Richardson number is given by:

$$L = \frac{Z_m}{R_i} \tag{3}$$

The equation 3 was used to estimate the approximate altitudinal height where free ascent destabilises forced ascent.

3.2.2. Estimation of Atmospheric Pressure and Potential Temperature

The calculated atmospheric pressure at vertical heights: 50m, 100m and 1300m were evaluated with the following equation:

$$P = P_0 \, e^{-(\frac{h}{h_0})} \tag{4}$$

Where,

P represents the atmospheric pressure (bars),

h, is the vertical height (km),

P_0, is the average mean sea level pressure

h_0 is a constant given as '7' (rough scale height for the atmosphere).

The potential temperatures (θ) of the air parcel at heights (50m, 100m and 1300m) were estimated with the following equation [23, 17].

$$\theta_z = T_z \, (\frac{P_s}{P})^{\frac{R}{C_p}} \tag{5}$$

Where, 'T_z' is the reference height temperature (K) 'R' is the gas constant of air and 'C_p' is the specific heat capacity of air at constant pressure. The fraction (R/C_p) is equal to '0.286'. At any height, z, there is a temperature value (T_z) and a resulting potential temperature (θ_z).

3.2.3. The Gradient Richardson Number as Stability Indicator

The gradient Richardson number (R_{ig}) is an important indicator of the level of stability conditions. The resolution of the scheme highlights the boundary limits of turbulence generated either by shear of buoyant forces and related to the stability regime of the sub-layers in the ABL. The R_{ig} has mostly been utilised as a measure for evaluating the stability of stratified shear flow [18]. Wind shear values [19] based on Richardson number has been related with atmospheric stability categories for Inland sites in Northeast region of Brazil (Table 1).

Table 1. *Atmospheric Stability on Wind Parameters in Northeast Brazil.*

Atmospheric Stability Group	R_i Values from Wind Shear
Very Unstable	0.14
Unstable	0.22
Near Neutral	0.36
Stable	0.38
Very Stable	0.34

Source: [19].

As noted by [20], Rig values between 0 and Richardson critical (R_{ic}) value (0.25), turbulent flow is generated mostly by forced convection. Negative R_{ig} values (both small and large) estimated in this study is classified as unstable conditions due to free convection [21]. Although it has been revealed that turbulence still exists in a weaker state for R_{ig} values greater than R_{ic} but lesser than the Richardson Termination (R_T) value of 1, the R_{ic} benchmark largely apply to the surface layer beneath 50m [16, 22]. This study considers the R_{ig} values within and above the R_{ic} limit as unstable and stable/neutral conditions as emphasised by [19] for in-land sites. An approximate vertical height where free convection interfered or completely displayed forced convection was as well computed in the study.

4. Results and Discussion

4.1. Variation of Gradient Richardson Numbers Across Specified Boundary Layers

The estimated average monthly gradient Richardson (R_{ig}) numbers for the specified layers within the ABL at the indicated synoptic hours are shown in Tables 2-4. In the first layer (10-50m) at the hours: 0000, 1200 and 1800, the dominant atmospheric conditions were stable from July-October; and neutral between June and September. Unstable conditions prevailed for the rest part of the periods (Table 2). Since all R_{ig} values across the specified hours were less than the Richardson Termination mark of 1, there is the likelihood that minimal levels of turbulence persisted during the periods when R_{ig} values were greater than R_{ic} of 0.25.

Table 2. *Gradient Richardson number Values in Jos for the Specified Layer/Hours.*

Month	0000HR				0600HR			
	Layer (m)	R_{ig}	Stability Pattern	Turbulence State	Layer (m)	R_{ig}	Stability Pattern	Turbulence State
JAN		0.07				0.07		
FEB		0.08				0.12		
MAR		0.07	Unstable	Turbulent		0.16		
APR		0.19				0.08		
MAY		0.09				0.17		
JUN	10-50	0.09			10-50	0.12	Unstable	Turbulent
JUL		0.29				0.17		
AUG		0.37	Stable	Laminar		0.09		
SEP		0.33				0.19		
OCT		0.48				0.19		
NOV		0.12	Unstable	Turbulent		0.12		
DEC		0.06				0.06		
	1200H				1800H			
JAN		0.05				0.06		
FEB		0.06				0.08		
MAR		0.10	Unstable	Turbulent		0.08		
APR		0.09				0.23	Unstable	Turbulent
MAY		0.18				0.12		
JUN	10-50	0.29	Stable	Laminar	10-50	0.18		
JUL		0.12				0.24		
AUG		0.14				0.24		
SEP		0.08	Unstable	Turbulent		0.33	Stable	Laminar
OCT		0.08				0.24		
NOV		0.09				0.08	Unstable	Turbulent
DEC		0.04				0.10		

The estimated R_{ig} numbers across the next sub-layer as shown in Table 3 i.e. (50-100m) have revealed an exclusively stable/neutral conditions as all values were above the R_{ic} limit of 0.25. Insignificant periods that had R_{ig} values lesser than the RT value of 1 across the hours indicated the times of insignificant turbulence within the layer (Table 3). The higher the positive R_{ig} values from the R_T mark of 1, the stronger the stable conditions.

Table 3. *Gradient Richardson number Values in Jos for the Specified Layer/Hours.*

Month	0000HR				0600HR			
	Layer (m)	R_{ig}	Stability Pattern	Turbulence State	Layer (m)	R_{ig}	Stability Pattern	Turbulence State
JAN	50-100	1.34	Stable	Laminar	50-100	1.29	Stable	Laminar
FEB		1.33				3.01		

Month	0000HR				0600HR			
	Layer (m)	R_{ig}	Stability Pattern	Turbulence State	Layer (m)	R_{ig}	Stability Pattern	Turbulence State
MAR	50-100	1.27	Stable	Laminar	50-100	1.28	Stable	Laminar
APR		1.27				1.93		
MAY		1.28				1.29		
JUN		3.02				0.90		
JUL		2.02				1.30		
AUG		3.60				2.04		
SEP		3.59				2.03		
OCT		3.56				3.59		
NOV		1.91				2.01		
DEC		0.89				0.91		
	1200H				1800H			
JAN		1.33				1.32		
FEB		1.31				1.31		
MAR		0.87				1.25		
APR		2.95				1.26		
MAY		5.27				2.97		
JUN		1.99				1.99		
JUL		2.01				5.36		
AUG		1.29				2.02		
SEP		2.00				3.57		
OCT		3.53				3.53		
NOV		0.65				1.26		
DEC		0.98				0.65		

Findings from the upper layer (100-1300m) as shown in Table 4 with greater altitudinal expanse than the other lower layers have revealed a strongly unstable conditions across the specified hours. All estimated R_{ig} numbers were generally negative and large. This indicates strongly unstable situations over the layer. Minimal or large negative R_{ig} numbers indicates unstable atmospheric conditions resulting from buoyant ascents [21, 23]. It has been disclosed [24] that for negative Rig values, turbulence results from both free and forced generated convection, but with more of free ascents.

Table 4. *Gradient Richardson number Values in Jos for the Specified Layer/Hours.*

Month	0000HR				0600HR			
	Layer (m)	R_{ig}	Stability Pattern	Turbulence State	Layer (m)	R_{ig}	Stability Pattern	Turbulence State
JAN	100-1300	-74.13	Unstable	Turbulent	100-1300	-90.44	Unstable	Turbulent
FEB		-98.88				-123.53		
MAR		-88.41				-98.88		
APR		-98.23				-110.40		
MAY		-110.13				-89.87		
JUN		-141.35				-68.28		
JUL		-183.84				-90.60		
AUG		-250.73				-125.60		
SEP		-359.93				-184.63		
OCT		-247.89				-249.53		
NOV		-122.87				-139.75		
DEC		-67.99				-74.95		
	1200H				1800H			
JAN	100-1300	-58.09	Unstable	Turbulent	100-1300	-67.34	Unstable	Turbulent
FEB		-66.18				-87.24		
MAR		-72.12				-87.08		
APR		-122.06				-136.61		
MAY		-208.45				-158.28		
JUN		-157.54				-210.57		
JUL		-123.59				-298.45		
AUG		-99.31				-249.45		
SEP		-110.13				-357.64		
OCT		-109.22				-245.82		
NOV		-52.06				-108.43		
DEC		-45.25				-61.56		

As revealed by [8], the boundary layer close to the earth surface layer is continuously dominated by significant scale of turbulence generated by buoyancy or forced ascents as well as both referred to as mixed convection while the next layer is majorly in a stable state. This stable layer creates a barrier between the surface and the upper atmosphere. Due to its location on the Plateau and the rough terrain, Jos is exposed to moderate to strong winds ranging from 2m/s to above 4m/s. This wind pattern regulates the intensity of thermal buoyancy especially during the day thereby enhancing forced convection at the surface layer.

Results from the monthly variation of stability conditions as shown in Figures 6-9 reveals that across the hours unstable conditions persist strongly from November to March at the surface layer (10-50m) as R_{ig} values were below the R_{ic} of 0.25.

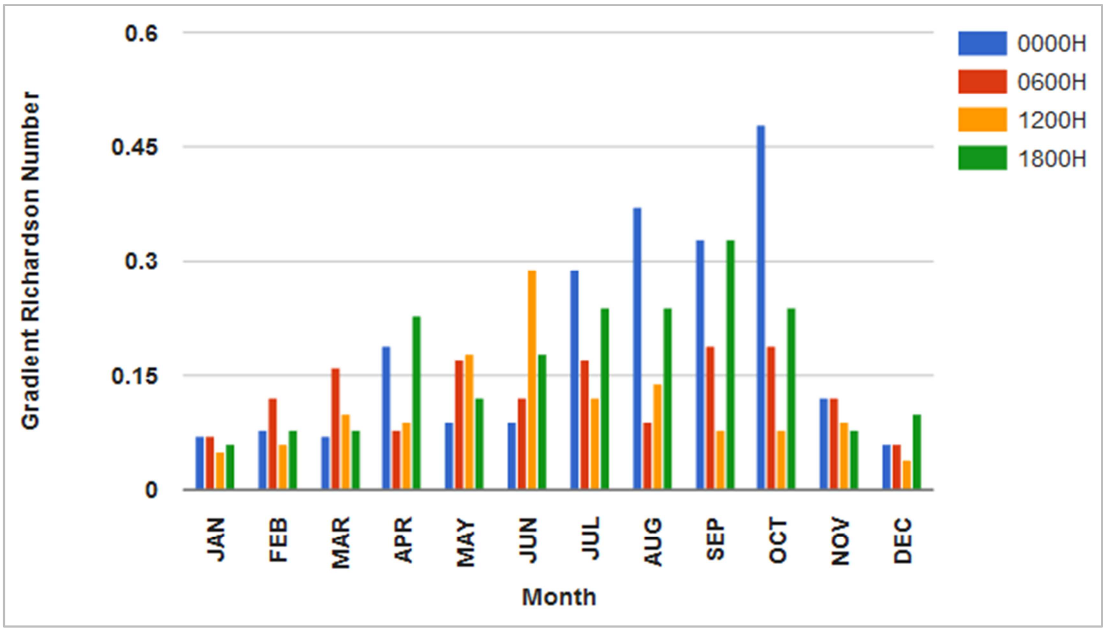

Figure 6. *Monthly R_{ig} Trend at 10-50m Layer for the Specified Hours.*

This period at the study area falls within the peak dry season when greater solar radiation is received; hence, mixed convection due to buoyancy and forced ascents would have acted together to energise instability. Findings during the rainy periods at the surface layer indicated levels of increased stability most especially at 0000H and 1800H. During these hours, thermal interference is insignificant to stimulate mixed convection.

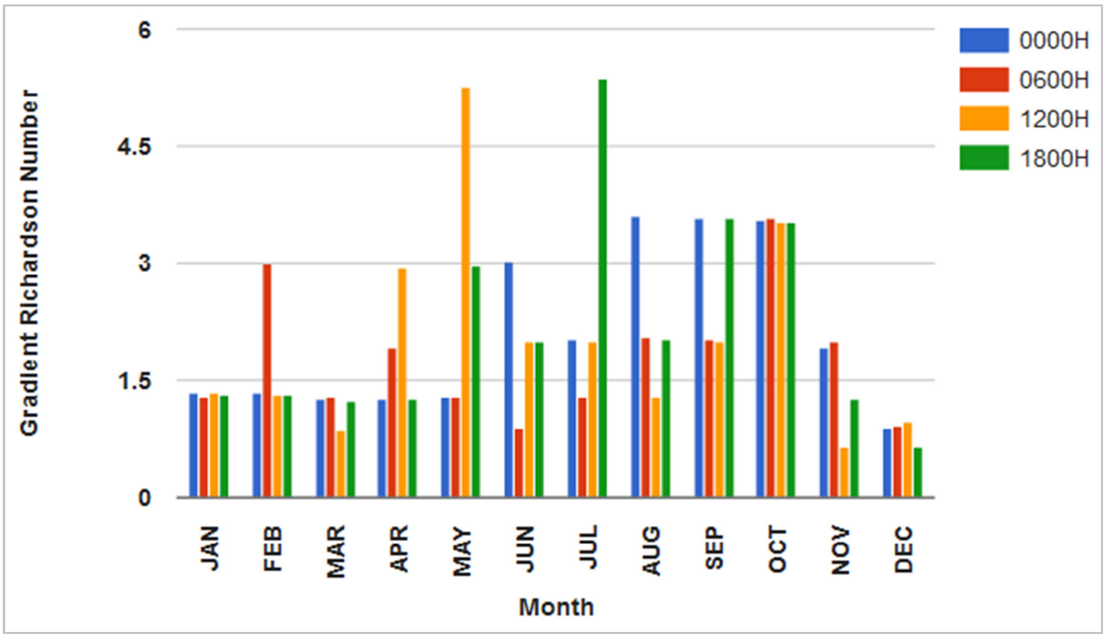

Figure 7. *Monthly R_{ig} Trend at 50-100m Layer for the Specified Hours.*

Regarding the more stable layer (50-100m) which acts as buffer zone, October indicated the more stable period while the hours: 1200 and 1800 in May and July showed greater stability than the rest periods. Overall, January, March and December were the least stable months; implying periods where intrusions of thermal buoyancy would have penetrated the layer.

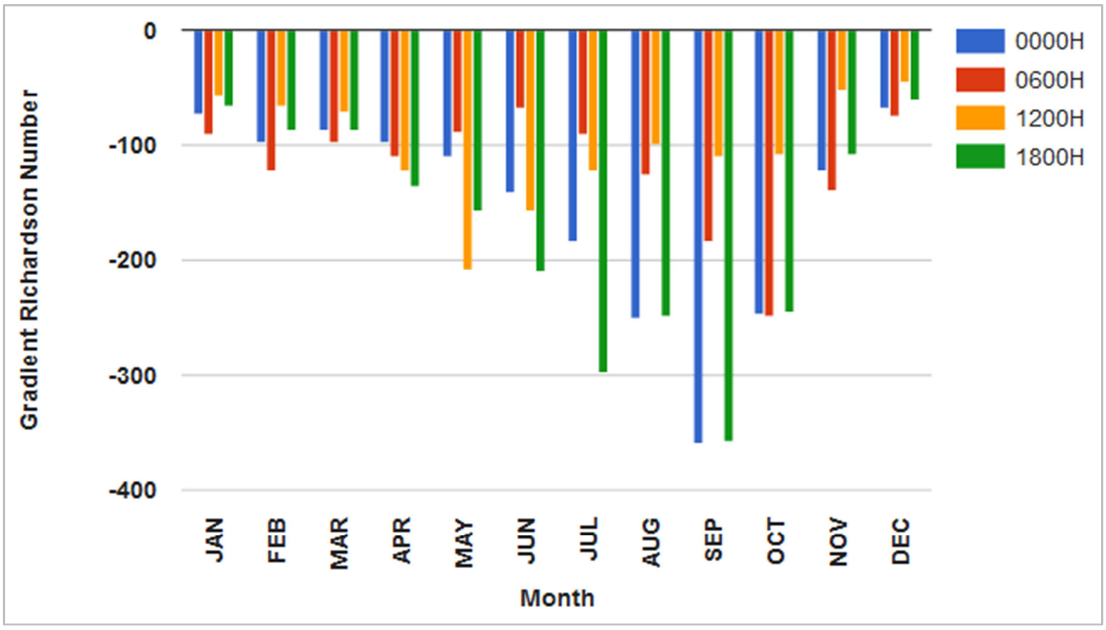

Figure 8. *Monthly R_{ig} Trend at 100-1300m Layer for the Specified Hours.*

At the upper layer (100-1300m) with elongated stretch, November to April exhibited average R_{ig} values below -150 across the hours while the other months had periods of larger R_{ig} values above -200. It has been indicated that larger negative R_{ig} values exhibit forced convection as a stronger influence for unstable conditions while smaller negative R_{ig} values has free convection as the stronger influence [21]. This suggests that for the months of November to April in the study area, unstable conditions were largely due to thermal buoyancy.

Findings from the analysed connection between Richardson number and Monin-Obukhov Length as revealed in Figure 9 shows that the average vertical distance where free convection dominates forced convection was below 240m, and that the average distance is lower during the peak rainy periods (July-September) than the peak dry periods (November-March).

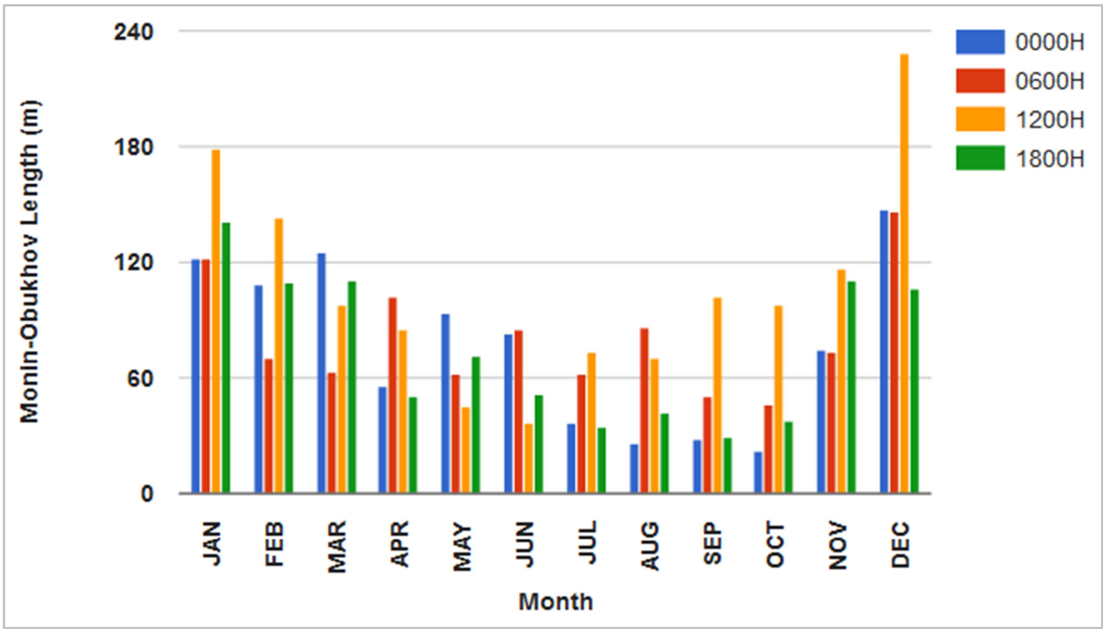

Figure 9. *Monthly Variations of Vertical Heights where Free Ascent Subverts Forced Ascent.*

4.2. Implications of Evaluated Stability Pattern on Emissions Dispersion

The R_{ig} assessment of the area shows the pattern of atmospheric stability boundary across the boundary layers. The ABL is crucial to determining air quality and determining the stages of stability amid layers goes to show the boundary limit and how pollutants are dispersed across layers [25]. Findings reveal that pollutant dispersions will be better at the surface layer and the upper layer due to their continuous state of instability whereas it will be stagnated at the laminar layer (50-100m). Nevertheless, the degree of instability at the upper layer of 100-1300m may create openings for the outflow of confined emissions from the stable layer. It was specified [26] that air mass transfer within the stable boundary layer is by conduction and altitudinal interactions of heat and moisture are very minimal.

While emissions from ground level sources will be dispersed within the layer, emissions from the upper level sources will be dispersed aloft. Ground level sources are those according to U.S. EPA, defined for stacks between 0 – 10m, while elevated sources are those defined for stacks between 10-200m and above. From the results, analysis of emissions dispersion at the surface layer will be better enhanced during the dry season (November-March) at the study area due to stronger instability pattern than the peak rainy periods (Figure 6). However, the stable condition of the mid-layer (50-100m) will limit emissions dispersion. Due to the strongly unstable nature of the upper layer (100-1300m), emissions will be dispersed aloft. At night when temperature inversion is more likely, emissions released from surface sources below 100m will increase ground level concentrations. The dispersion of air pollutants during the inversion period will however now depend on the magnitude of wind force. Significant amount of turbulence still exists during the 0000H in Jos due to mechanical turbulence and this could be vital in moderating pollutant concentrations during inversion periods at night. As the night progresses, inversion could become stronger at the surface and therefore limit pollutant dispersion. The turbulent pattern at the upper layer (100-1300m) will be substantial in moving released air pollutants from emission sources above 100m across borders as dispersions take place above the stable layer (50-100m). This could impact on distant receptors by gravitational settling at the breaking of the inversion layer during the day or by high pressure subsidence that characterises the study area as a result of the undulating terrain.

5. Conclusions

Atmospheric stability within the planetary boundary layers affects both weather processes and human activities and Jos; an urban centre located in north-central Nigeria reacts to such realities. The degree of atmospheric stability conditions across three different vertical layers (10-50m; 50-100m and 100-1300m) at the study area was conducted using the gradient Richardson number (R_{ig}) technique for the synoptic hours: 0000H, 0600H, 1200H and 1800H. The gradient Richardson number is a widely used technique in accessing the degree of turbulence that enhances stability conditions within the boundary layer. Its level of applicability and accuracy pivots on the extent of acceptability across boundary layer studies. Findings show that at the surface layer (10-50m), significant level of instability exists largely due to forced convection. Although over 90% of R_{ig} values at this layer were below the critical Richardson number (R_{ic}) of 0.25, all values were lesser than the R_T level of 1 and boundary layer researchers maintains that levels of instability still occurs for all R_{ig} values less than 1 [16, 22], even though the effect is more significant below the critical level. Also, R_{ig} findings show that the mid layer (50-100m) portrays stable condition as all R_{ig} values were greater that the R_T level of 1. However, the condition at the upper level (100-1300m) indicated strongly unstable conditions throughout the hours and periods considered as R_{ig} values were mainly negative with range -52 to -360. It is highlighted that both thermal and mechanical turbulence contributes to negative R_{ig} values. Large negative R_{ig} values are due to more of mechanically generated turbulence, while small values are due to more of thermal turbulence.

Atmospheric stability due to mixed convection was prevalent in the study area. Whereas instability generated by mechanical turbulence was more prominent at the surface, that generated by thermal turbulence more in the upper layer. The mechanical or forced ascent induced stability pattern could result from the undulating terrain that creates wind shear thereby forcing air mass upwards. Thermal or free ascent can also induce stability pattern at the upper layer, which could result from latent heat releases from rising air mass that creates instability. It could also result from the interactions of high and low pressure areas generated by the topographic pattern of the study area. The atmospheric stability pattern at the area proposes that emissions will be transported to distant receptors at the upper layer due to the stable nature of the mid layer. Also, emissions will be dispersed within the surface layer if the emission sources are below 50m. Nevertheless, if the emission sources are above 50m, emission dispersion will take place aloft. Findings also suggest that wind turbines development for power generation will be suitable within the surface layer when R_{ig} values are compared to values generated in northeast Brazil.

References

[1] Hutschemaekers, J. J. N. (2014). Comparison of Classification Systems to define Atmospheric Stability and their impact on Wind Turbine Design. A Published Master of Science Thesis from the Delft University of Technology, The Netherlands. September 8.

[2] Ashrafi, K. and Hoshyaripour, G. A. A model to determine atmospheric stability and its correlation with CO concentration. *International Journal of Civil and Environmental Engineering*. 2 (2), 82-88. 2010.

[3] Koblitz, T., Bechmann, A., Berg, J., Sogachev, A., Sørensen, N and Réthoré, P-E. Atmospheric stability and complex terrain: comparing measurements and CFD. *Journal of Physis*. 555 (1), 1-11. 2014.

[4] Jayasudha, G. T., Vijayakumar, B., Ravi, P. M., Bhatt, B. C., and Kulkarni, M. S. (Eds.). A case study of atmospheric stability pattern at Kudankulam site and its correlation with suspended particulate matter. India: Bhabha Atomic Research Centre. 2014.

[5] Lanigan, D., Stout, J. and Anderson, W. Atmospheric stability and diurnal patterns of Aeolian saltation on the Llano Estacado. *Aeolian Research*. 21 (2016), 131-137.

[6] Newman, J. F. and Klein, P. M. (2014). The impacts of Atmospheric Stability on the Accuracy of Wind speed Extrapolation Methods. *Resources*, 3, 81-105. Doi: 10.3390/resources3010081.

[7] Arya, P. (1998). *Introduction to Micrometeorology*, 2nd Edition. San Diego: Academic Press.

[8] Oke, T. R. (1987). *Boundary Layer Climates*, 2nd Edition. Lagos: Methuen Publishers.

[9] Mikkelson, T. (2003). Modeling of Pollutant Transport in the Atmosphere. Atmospheric physics division, wind department, Risq National Laboratory, Denmark.

[10] Stull, R. B. (2012). *An Introduction to Boundary Layer Meteorology*. Netherland: Springer. Available from: https://books.google.com.ng/books?id=2PjrCAAAQBAJ&dq =boundary+layer+turbulence&source=gbs_navlinks_s

[11] Agbo, G. A. (2011). Tropospheric Refractivity Dependence on Atmospheric Weather Conditions in Jos Nigeria. *Journal of Basic Physical Research,* 2 (1), 1-6. Available from: http://www.jbasicphyres-unizik.org/files/2011files/1-Basic%20Correct.pdf

[12] Ajuzie, C. C. (2012). A First Survey of Phytoplankton Community Richness in Lamingo Reservoir, Jos, Nigeria: A Wake-up Call for the Continuous Monitoring of Microalgae in Surface Waters Serving as Drinking Water Sources in Nigeria. *New York Science Journal,* 5 (2), 1-8. Available from: http://www.sciencepub_new_york_science_journal.pdf.

[13] Jos climate history (2016). Retrieved from http://www.myweather2.com/City-Town/Nigeria/Jos/climate-profile.aspx

[14] Idris, N. A., Lamin, H. S., Ladan, M. J. and Yusuf, B. H. (2012) Nigeria's Wind Energy Potentials: the Path to a Diversified Electricity Generation-Mix. *International Journal of Modern Engineering Research (IJMER)*, 2 (4) 2434-2437.

[15] Lawal, J. R., Bello, A. M., Balami, S. Y., Dauda, J., Malgwi, K. D., Ezema, K. U., Kazim, M. and Biu, A. A. (2016). Prevalence of Haemoparasites in Village Chickens (*Gallus gallus domesticus*) Slaughtered at Poultry Markets in Maiduguri, North-eastern Nigeria. *Journal of Animal Science and Veterinary Medicine*, 1, 39-45. Available from: http://www.integrityresjournals.org/jasvm/publications/2016/pdf/04lawal%20et%20al.pdf

[16] Stull, R. B. (1988).*An Introduction to Boundary Layer Meteorology*. Netherland: Springer.url={https://books.google.com.ng/books?id=BK8P9rl- CB4C}.isbn={9789027727688}, lccn={88015564}.

[17] Ward, D. (2012). ATMO 336: Weather, Climate and Society. Department of Atmospheric Science, University of Arizona. Lecture Training Materials.

[18] Gastel, P. V. and Pelegri, J. L. (2004). Estimates of gradient Richardson numbers from vertically smoothed data in the Gulf Stream region. *SCI. MAR.,* 68 (4), 459-482.

[19] Vieira, C. F. A. and Sampaio, E. F. (2012). Analysing the impact of atmospheric stability on wind parameters in North East Region of Brazil. Brazil Wind Power. Siemens Energy International, August 29 and 31.

[20] Murty, K. P. R. V., Filho, E. P. M., Prasad, G. S. S. D. and Deane de Abreu Sá, L. (1998). Intercomparison of Flux, Bulk and Gradient Richardson Number and its Spatial and Temporal Variation as Revealed by Interdisciplinary Pantanal Experiment (IPE-1). http://www.academia.edu/20968829/Intercomparison_of_flux_bluk_and_gradient_Richardson_number_and_its_spatial_and_temporal_variation_as_revealed_by_interdiciplinary_Pantanal_experiment_IPE-1_may_1998

[21] Jacobson, M. Z. (1999). Fundamentals of Atmospheric Modelling. Cambridge: University Press. url={https://books.google.com.ng/books?id=QnzHkFN3v8AC}isbn={9780521637176}, lccn={98015180}.

[22] Grachev, A. A., Andreas, E. L., Fairall, C. W., Guest, P. S. and Persson, P. O. G. (2012). The Critical Richardson Number and Limits of Applicability of Local Similarity Theory in the Stable Boundary Layer. *Boundary Layer Meteorology*. Available from: https://arxiv.org/ftp/arxiv/papers/1202/1202.5066.pdf.

[23] Bailey, D. T. (2000). Meteorological monitoring guidance for regulatory modelling applications. U.S Environmental Protection Agency. Office of Air and Radiation; Office of Air Quality Planning and Standards. url={https://books.google.com.ng/books?id=_86ik7kVtAUC}, lsbn= 9781428901940.

[24] Kaimal, J. C. and Finnigan, J. J. (1994). Atmospheric Boundary Layer Flows: There Structure and Measurement. New York: Oxford University Press. 289pp.

[25] Eresmas, N., Harkonen, J., Joffre, S. M. Schultz, D. M., Karppinen, A. and Kukkonen, J. (2012). A Three-Step Method for Estimating the Mixing Height Using Ceilometer Data from the Helsinki Test bed. Journal of Applied Meteorology and Climatology, 51, 2172-2187. DOI: 10.1175/JAMC-D-12-058.1

[26] Ayoade, J. O. (2004). *Introduction to Climatology for the Tropics* (2nd Edition). Ibadan: Spectrum Books.